

CHAPTER  
**35**

# Pediatric Applications of Perfusion Ultrasound

Q1

Karl Muchantef, Thomas Scholbach, and Ricardo Faingold

Q2

## ■ Introduction

Knowledge of blood flow and tissue perfusion can influence clinical decisions and patient management in a gamut of disease processes. Many diseases are associated with perfusion changes, such as inflammatory processes, organ failure, transplant rejection, arterial stenosis, tumor growth and necrosis, hypoperfusion, and ischemia. The Doppler shift of ultrasound (US) frequency can be used to depict blood flow velocity and to quantify it. US and Doppler techniques are currently very popular and have many advantages over other modalities with potential in perfusion mapping: computed tomography (radiation exposure), magnetic resonance imaging (cost, availability, length of exam, sedation in young children), and nuclear medicine (limited morphologic information, radiation).

Several publications using color Doppler sonography (CDS) assessed quantification of tissue perfusion by counting color Doppler signals in still images.<sup>1-3</sup> There are also reports on the use of quantitative Doppler signal analysis with and without contrast-enhancing agents.<sup>4-9</sup> Despite such developments, it is not a simple task to obtain blood flow and tissue perfusion data in a reliable, noninvasive, inexpensive, and radiation-free manner. This chapter discusses the most currently used Doppler techniques (color Doppler, power Doppler, pulsed Doppler, and contrast-enhanced US) and also the potential of perfusion quantification with dynamic CDS or dynamic tissue perfusion measurement (DTPM) in children. Spectral Doppler velocity measurements and resistive index (RI) are still the basis of many scientific medical investigations of perfusion, despite offering a limited representation of actual tissue perfusion, as detailed below.

Q3

## ■ Color and Power Doppler

Color Doppler uses red and blue shades to depict blood flow toward or away from the transducer (according to equipment settings), with differing shades representing differing velocities of motion. The color hue assigned to a pixel results from the angle-dependent Doppler frequency shift returning from that pixel. By convention, higher velocities of blood flow are assigned a brighter color hue. The measured US frequency shift is displayed as an array of colors within a gray-scale image, depicting the local velocity of blood flow. Color Doppler hence provides an image with tissue morphology depicted in gray scale and blood flow depicted by color.<sup>10,11</sup> Power

Doppler imaging depicts the strength of the Doppler-shifted signal rather than the frequency shift of that signal. That is to say, the color hue depicted relates mainly to the volume of moving blood, rather than the velocity and direction of the flow. Directional information is lost in power Doppler imaging; its advantage is increased sensitivity to low flow as compared to color Doppler.<sup>11</sup>

## ■ Spectral Doppler

In the case of spectral Doppler imaging, a time velocity tracing depicts variations in blood flow velocity at a point within a vessel during the cardiac cycle. Spectral Doppler analysis has gained tremendous popularity and found many clinical applications. Using the spectral tracing, the RI may be calculated from the equation:

$$RI = (PSV - EDV) / PSV,$$

where PSV is the peak systolic velocity, and EDV is the end-diastolic velocity. This ratio describes the relative degree of velocity drop during a complete heart cycle. The RI calculation is independent of the angle of insonation; the RI expresses the ratio of two velocities, both identically affected by the Doppler angle.

The RI is sometimes interpreted as a parameter of blood flow itself. It is often assumed that a high RI signifies a low perfusion state and an increasing RI indicates decreasing perfusion; however, this is not necessarily the case.<sup>12</sup> RI relies upon only two velocity measurements (PSV and EDV) obtained at a single point in a single vessel. As a surrogate measure of tissue perfusion, RI measurements disregard a crucial point: tissue viability depends not only on the pulsatility of blood flow or the resistance against it but also on blood flow volumes (Table 35.1).

Table 35-1

## ■ Contrast-Enhanced Ultrasound

Microbubble-based intravenous contrast agents are not routinely used in pediatric imaging in North America. Intravenously injected microbubbles enhance US backscatter by producing harmonic frequencies that are multiples of the transmitted frequency and therefore increase the US signal from flowing blood, particularly in the arterial system and microvasculature.<sup>10</sup> Level of saturation and velocity to reach the level of saturation are obtained with dedicated software. Contrast-enhanced ultrasound (CEUS) has many clinical applications,<sup>13-15</sup> some of which are discussed later (Table 35.2).

TABLE	
<b>35.1</b>	<b>Resistive Index</b>
Measures one point in one vessel	
Velocity information usually available	
Cardiac cycle dynamics preserved	
Noninvasive	
Unlimited observation time	
Inexpensive	
Fast acquisition	

### Dynamic Tissue Perfusion Measurement

A software-based DTPM technique is capable of extracting dynamic (changing with heart cycle) flow data of perfusion signals from color Doppler sonographic videos. Perfused area and actual local perfusion velocity within an arbitrarily chosen region of interest (ROI) are extracted automatically by software from a sonographic video (PixelFlux, Chameleon-Software, Leipzig, Germany).<sup>16</sup> No ECG gating is required, and the software recognizes the variation of flow and is able to establish the cardiac cycle based on a pattern.

The guiding idea behind DTPM is to quantify tissue perfusion by referring to all relevant parameters that influence the total amount of blood passing through a tissue section during a complete heart cycle. These are the mean perfusion velocity of all vessels and the mean perfused area of the tissue section under investigation. Both are directly proportional to the amount of transported blood. Both do also change significantly during one complete cardiac cycle. It is therefore necessary to start with the measurement of these two basic parameters at the beginning of a heartbeat and to continue in as short time intervals as possible to the end of the heartbeat. This is important because significant differences between momentary systolic and diastolic perfusion may exist even in tiny vessels.

From these data, a mean perfusion velocity, as well as a mean perfused area, are calculated thus referring all measurement to the very basic rhythm of perfusion—one complete heart cycle. By multiplication of these mean values—mean perfused area and mean perfusion velocity—mean perfusion intensity is calculated. Mean perfusion intensity thus also refers to the area of the tissue section that is captured by the ROI of the current investigation: mean velocity (*v*) of all pixels is multiplied by the area (*A*) of all

Q4

TABLE	
<b>35.2</b>	<b>Contrast-Enhanced Ultrasound</b>
Measures enhancement in an ROI	
Velocity information not available	
Cardiac cycle dynamics not preserved	
Invasive	
Limited observation time	
Expensive	
Slow acquisition, requires postprocessing	

colored pixels contained with the ROI and divided by the total area of the ROI (colored pixels plus gray-scale area of nonperfused tissue). Thereby, the mean flow intensity value of the ROI (*I*) is calculated.

$$I[\text{cm/s}] = A[\text{cm}^2] \times v[\text{cm/s}] / A_{\text{ROI}}[\text{cm}^2]$$

Following this algorithm, a dynamic (with respect to the ever-changing values during a full heart cycle) mean perfusion intensity can be calculated of a tissue section in a freehand or geometrically standardized ROI (Fig. 35-1).

Fig. 35-1

As with any measurement, a crucial point is standardization—in DTPM, it is the presetting of the US equipment. Color Doppler frequency as well as gain have to be kept constant for comparable investigations. Color flow velocity settings may be changed to avoid aliasing if necessary. The software recognizes the change of color scale values automatically (Table 35.3).

### Practical Issues Regarding DTPM

Spectral Doppler, color Doppler, and power Doppler sonography are often used to assess blood flow and provide an estimate of organ perfusion. Quantitative evaluation of blood flow with CDS using pixel count per square centimeter has been described in assessment of bowel perfusion.<sup>12</sup> There are also reports on the use of quantitative Doppler signal analysis with and without contrast-enhancing agents.<sup>5-9</sup> However, it may be time-consuming and difficult to reproduce in the clinical and research settings. Evaluation of Doppler spectral waveform is helpful in determining the characteristics of blood flow patterns, which are affected by the metabolic status of the organ supplied by that vessel, hemodynamic status, and age of the patient.<sup>17</sup> DTPM offers a standardized, quantitative assessment of tissue perfusion within a definable ROI. Data are extracted over the cardiac cycle and flow parameters obtained.

### Applications of Doppler US and DTPM

To demonstrate the broad applicability of Doppler US and DTPM, some examples of clinical applications are given below in infants, children, and adolescents.

#### Infants

Assessment of blood flow and organ perfusion in infants has been traditionally done by spectral Doppler and sometimes by CDS.<sup>2,17,18</sup> Recent use of CDS with tissue perfusion quantification has shown that this technique is promising and with great potential as a noninvasive tool in the research setting and clinical practice.<sup>19,20</sup>

#### Kidneys

The use of RI is well established in the evaluation of the kidneys. It is well known that RI of renal arteries varies in the first 12 months of life. They are usually measured in the arcuate or interlobar arteries. In term infants, the RI ranges from 0.6 to 0.8, although in premature babies, RI may reach 0.9 in the renal arteries. The hemodynamic status and the structural and functional immaturity of the kidneys in neonates are responsible for these changes.<sup>17</sup>

Acute kidney injury (AKI) has been associated with perinatal asphyxia, hypotension, or cardiac failure. It may develop with or without changes in creatinine levels or urine output. Decreased blood flow velocity in the renal arteries with pulsed Doppler imaging has been described in severe hypoxic-ischemic injury (HII).<sup>3</sup> CDS evaluation of renal parenchyma<sup>20</sup> appears to be a useful tool for quantification of renal perfusion in AKI (Fig. 35-2).

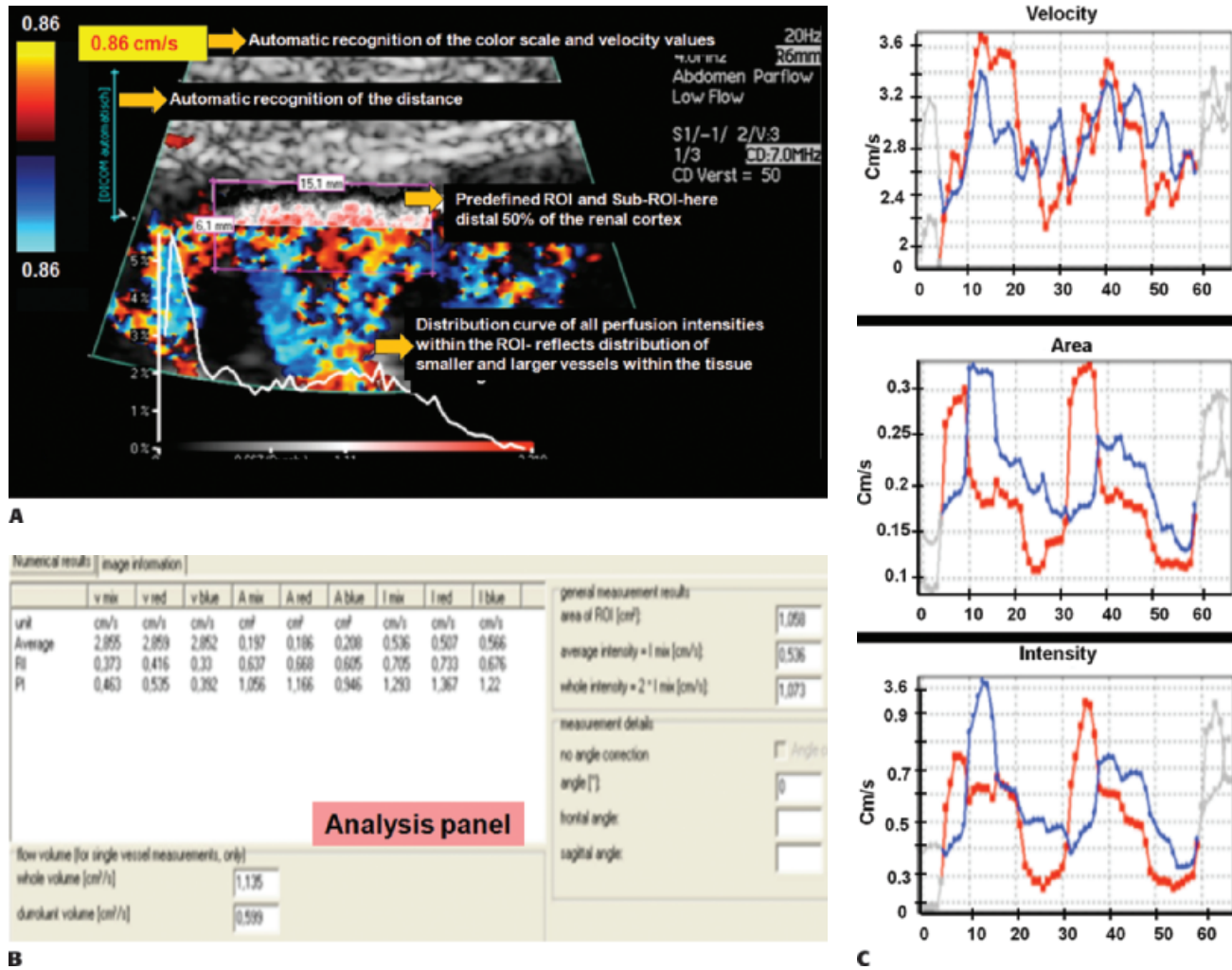


**Figure 35-1.** Tissue perfusion of the renal cortex. **A:** A standardized region of interest (ROI) is defined with a sub-ROI defining the distal 50% of the cortex. Each ROI contains colored pixels and nonperfused tissue. Numerical description of vessel distribution according to their perfusion intensities with associated distribution curve is included (*white curve*). **B:** Tables of dynamic tissue perfusion measurement (DTPM) results are shown in analysis panel and in **(C)**. Time course diagrams of relevant perfusion parameters (*graphs*).

**Bowel**

US Doppler interrogation of the gastrointestinal tract is useful for assessment of superior mesenteric artery (SMA) Doppler waveform and intestinal perfusion. The flow pattern in the SMA is of high

resistance in the fasting state and becomes of low resistance with loss of reversal of diastolic flow in the postprandial state.<sup>17</sup> In normal fasting neonates, bowel wall perfusion usually ranges from one to nine color Doppler signals per centimeter square (mean = 3.78, standard error of mean = 0.20).<sup>2</sup>

TABLE

**35.3 Tissue Perfusion Measurement**

- Measures perfusion of all vessels in an ROI
- Velocity information available
- Cardiac cycle dynamics preserved
- Noninvasive
- Unlimited observation time
- Inexpensive
- Fast acquisition, requires postprocessing

**Necrotizing Enterocolitis**

Intestinal mural perfusion can be assessed directly, in real time at the bedside, with CDS. In 2005, the use of color Doppler was described to assess bowel wall perfusion in necrotizing enterocolitis (NEC).<sup>2</sup> In neonates with NEC, color Doppler US revealed three types of flow in the bowel wall: normal, increased, and absent. Normal CDS flow corresponded to the values obtained in control infants. CDS flow was considered increased when certain types of hyperemic flow pattern were different from the normal neonates. They were described as follows: “circular” flow pattern around the bowel; a “Y” pattern of distal mesenteric and subserosal vessel; and parallel CDS lines or a “zebra” pattern due to increased flow in mucosal folds. CDS perfusion was considered absent when no mural CDS signals were demonstrated (Fig. 35-3). These nonperfused bowel loops were correlated with abdominal x-rays (AXR) and with laparotomy and

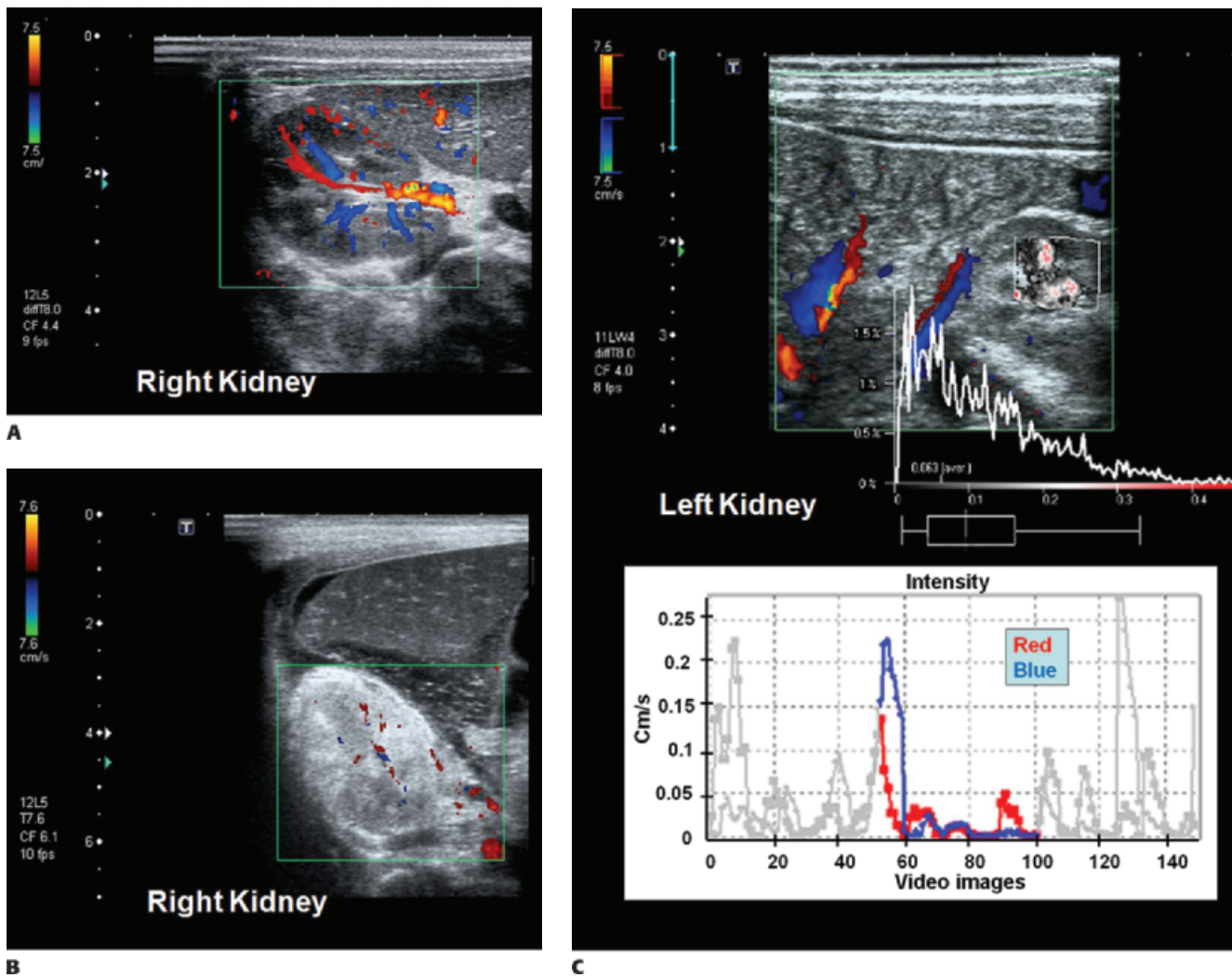


**Figure 35-2.** Renal perfusion with color Doppler sonography (CDS). **A:** A 2-day-old boy. Perfusion with CDS shows normal parenchymal flow. **B:** A 1-day-old boy. CDS shows decreased perfusion within hyperechogenic parenchyma. **C:** A 2-day-old girl. DTPM with quantification of ROI using dedicated software and renal perfusion intensity curve shows values of 0.15 cm/s, indicating preserved flow. *Red* and *blue* curves represent blood flow toward and away from transducer during dynamic CDS measurements.

pathologic specimens. The sensitivity of CDS to detect gangrenous bowel was 100% compared to 40% for AXR.<sup>2</sup>

### Intestinal Hypoxic–Ischemic Injury

Asphyxia may result in perinatal hypoxia, hypercarbia, and acidosis. It may cause redistribution of blood flow with an increase in the flow to the brain, heart, and adrenal glands and a decrease to the kidneys, bowel, and skin. Multiple organ failure has been reported in more than 50% of infants with severe perinatal asphyxia.<sup>18</sup>

It has been reported that pulsed Doppler interrogation in the SMA is altered in neonates with perinatal asphyxia. They showed a significant decrease in the mean blood flow velocities and increase in RI in severe HII.<sup>18</sup>

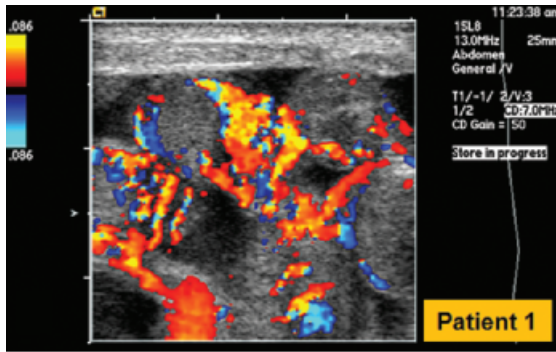
Evaluation of intestinal mural blood flow with CDS and dynamic CDS or DTPM has been described as preserved intramural perfusion and increased or decreased bowel perfusion. In a retrospective pilot study, we evaluated 28 neonates using DTPM. We were able to assess intramural perfusion of a specified ROI and observed a trend toward a decreased bowel wall perfusion

(Fig. 35-4) during the first 24 hours of life in 7 nonsurvivors compared to 21 survivors ( $0.040 \pm 0.015$  cm/s  $\times$   $0.052 \pm 0.029$  cm/s).<sup>21</sup>

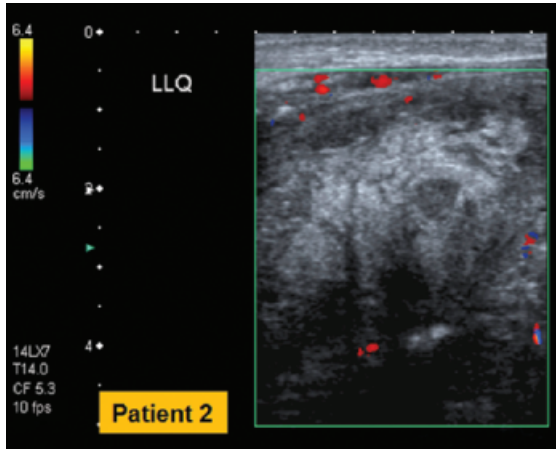
Therefore, assessment of the mesenteric circulation and bowel perfusion in perinatal asphyxia may have a role in predicting outcomes and understanding the pathophysiology of bowel injury in HII.

### Brain

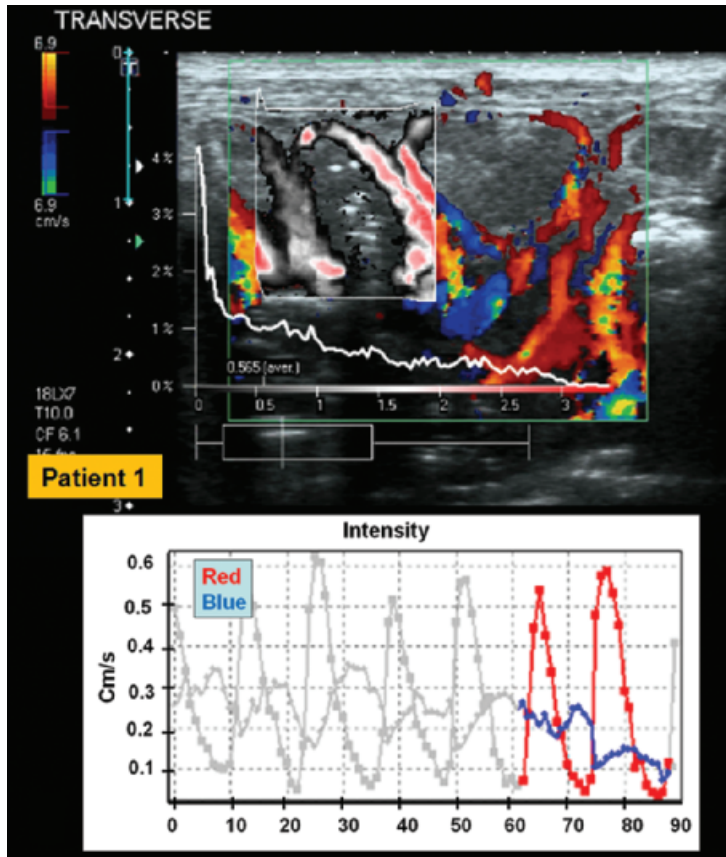
Normal cerebral blood flow (CBF) changes over time particularly in neonates. Cerebral perfusion corresponds to up to 25% of cardiac output in healthy infants. CBF is affected by cardiac output and also with variations of pO<sub>2</sub> and pCO<sub>2</sub>, for example, patients with patent ductus arteriosus may have CBF changes according to the severity of the disease. There is a physiologic increase in CBF during the first days of life, with corresponding increase in PSV and EDV. In premature neonates, resistive indices are known to be higher than in term neonates. The normal RI of intracranial arteries in term infants in the first day of life has been described to be 0.726 with a standard deviation of 0.057.<sup>22</sup>



**A**



**C**



**B**

**Figure 35-3.** Ultrasound images of the intestine in neonates with necrotizing enterocolitis (NEC). **A:** High-resolution CDS transverse image shows mixed pattern with “circular” and “zebra” patterns due to viable hyperemic perfusion pattern in bowel loops. **B:** DTPM with quantification of ROI using dedicated software and intestinal perfusion intensity curve shows values of 0.6 cm/s, indicating hyperemic flow in NEC. The patient did well clinically. **C:** Different patient: CDS transverse image shows featureless loops of bowel with absent perfusion in a premature baby with severe NEC confirmed by laparotomy to be gangrenous bowel.

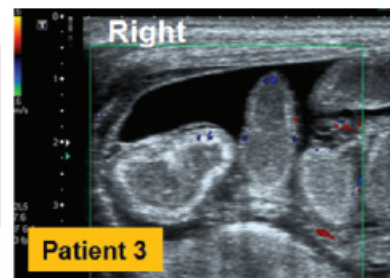
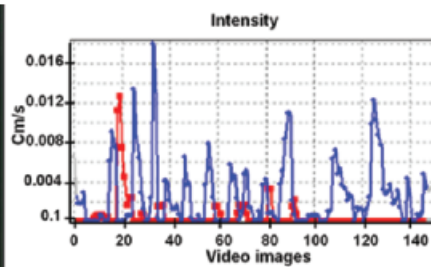
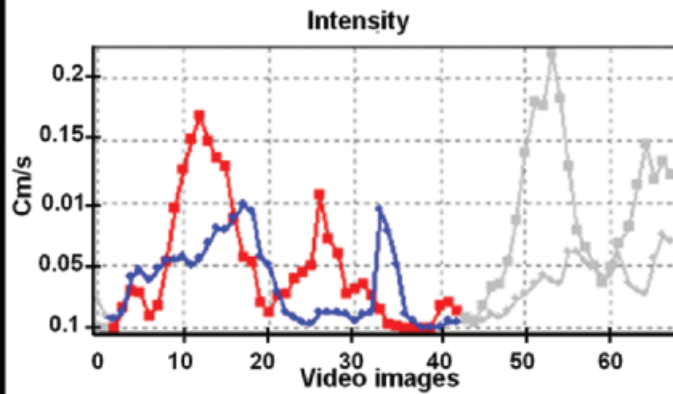
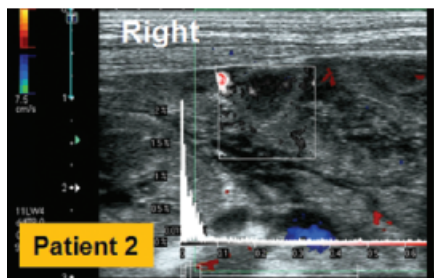
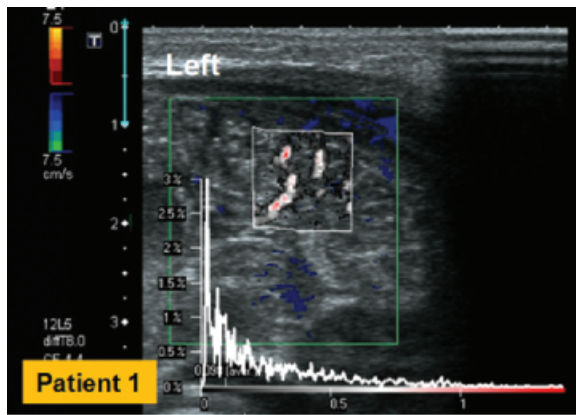


**Figure 35-4.** Intestinal color Doppler sonography and hypoxic-ischemic injury (HII). Patient 1 (*upper row*), a 1-day-old girl; DTPM demonstrates preserved bowel wall flow with quantification of ROI using dedicated software. Intestinal perfusion intensity curve with values of up to 0.17 cm/s. Patient 2 (*lower row*), a 2-day-old boy; DTPM shows decreased perfusion and corresponding intestinal perfusion intensity curve with values of up to 0.013 cm/s. Patient 3 (*lower row*); CDS shows some decrease in bowel perfusion and edematous bowel wall with associated ascites in a different infant.

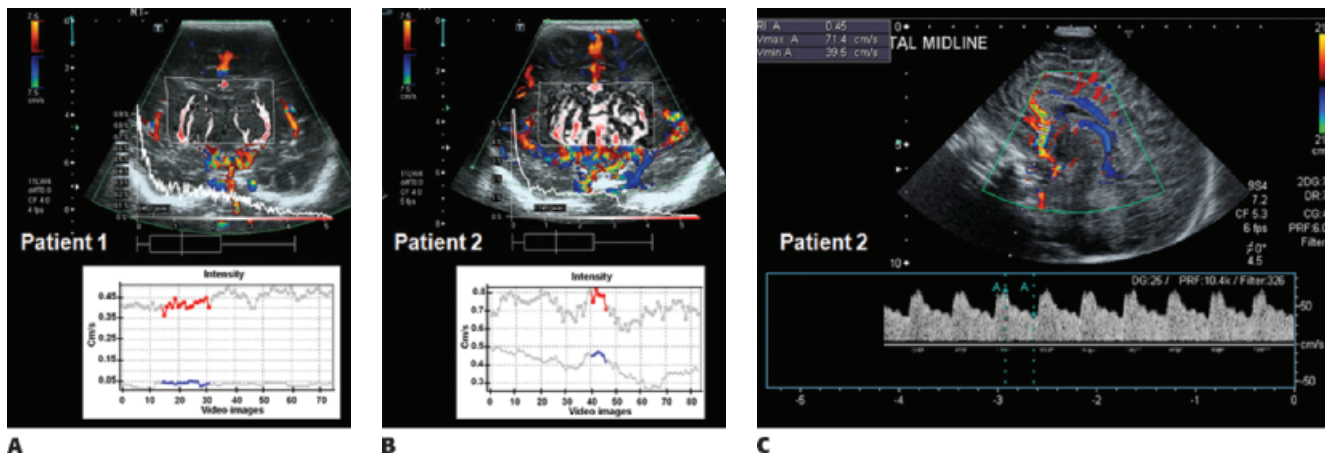


**Figure 35-5.** Hypoxic-ischemic encephalopathy (HIE) in two patients. **A:** Patient 1: A 1-day-old boy with mild HIE. DTPM shows ROI in basal ganglia to calculate cerebral perfusion intensity, and corresponding perfusion intensity curve with perfusion up to 0.45 cm/s. **B,C:** Patient 2: A 1-day-old girl with severe HIE. **B:** DTPM demonstrates very increased perfusion in basal ganglia (0.9 cm/s). **C:** Demonstrates pulsed Doppler interrogation with decreased intracranial resistive index (RI) in neonate with severe HIE.

### Perinatal Asphyxia and Hypoxic-Ischemic Injury

The causes of hypoxic-ischemic encephalopathy (HIE) are complex and related to multiple factors. They are thought to be due to changes in CBF by a combination of systemic hypotension, abnormal cerebral autoregulation leading to cerebral hypoperfusion, and subsequent HII.<sup>18,20</sup> During the postasphyxiated period, an increase in CBF within the first few hours of life may last for hours or days. This period is known as reperfusion phase and may be responsible for reperfusion brain injury.

In neonates with HIE, increased CBF velocities up to three times more than controls with decrease in RI of the intracranial arteries to 0.5 or less, measured at 12 to 72 hours of life, have been described in severe HII.<sup>18,23</sup> In a retrospective pilot study,<sup>19</sup> cerebral perfusion intensity with DTPM of basal ganglia values were significantly higher in the 7 nonsurvivors (Fig. 35-5) compared to 23 survivors ( $0.226 \pm 0.221$  vs.  $0.111 \pm 0.082$  cm/s;  $p = 0.02$ ). In neonates, at risk for stroke, CDS may also be used for assessment of luxury perfusion.

## Children and Adolescents

### Kidneys

Normally, the peak systolic flow velocity in the main renal arteries should be up to 180 cm/s, with diastolic forward flow of 25 to 50 cm/s.<sup>17</sup> At the renal parenchyma, there should be a brisk systolic upstroke with an acceleration index of greater than 300 cm/s<sup>2</sup>. Most consider that children older than 1 year have an RI similar to that of normal adults, 0.5 to 0.7, though some suggest that adult values are realized later in childhood.<sup>24,25</sup>

### Renal Artery Hypertension

Hypertension in children is usually secondary to parenchymal renal disease or lesions of the renal artery itself, with fibromuscular dysplasia as the most common cause of renal artery disease in children.<sup>26-28</sup> Additional causes of pediatric renin-angiotensin-mediated hypertension include inflammatory arteritis, congenital aortic coarctation, and extrinsic arterial compression (as may be seen with neurofibromatosis type 1), among others.

Imaging of the main renal artery for hypertension has focused on two parameters: PSV and renal-to-aortic velocity ratio. As mentioned, 180 cm/s is considered the upper limit for normal PSV.

A ratio of 3.5 is considered the upper limit for the normal renal artery-to-aorta ratio.<sup>17</sup> These criteria are well established in adult populations, though their diagnostic performance is largely unknown in children.

Spectral Doppler imaging at the level of the renal parenchyma is also performed routinely. The parameters of interest here are acceleration time and RI, as detailed above. These parameters may be limited by their normal variability in health kidneys.<sup>29,30</sup> While the role of US in the evaluation of pediatric renal artery stenosis remains controversial,<sup>31</sup> a recent study of 35 pediatric patients found a sensitivity of 90% and specificity of 68% for detecting a vascular cause for hypertension in high-risk individuals when an intrarenal RI of less than 0.5 or a tardus-parvus waveform was identified<sup>32</sup> (Fig. 35-6).

Contrast-enhanced US has been studied in adult populations for the diagnosis of renal artery stenosis.<sup>33,34</sup> Studies suggest that with the addition of contrast agent, the positive and negative predictive values of US in these patients are increased. DTPM may also contribute to the diagnosis of renal artery stenosis as diminished perfusion may be demonstrated at the level of the renal cortex, where the renin-secreting juxtaglomerular apparatus is located (Fig. 35-6).

### Renal Transplantation

The normal RI of a transplanted kidney in a pediatric recipient is 0.5 to 0.8.<sup>35</sup> When grafting adult kidneys into pediatric patients, an inverse correlation between size of the recipient and the RI was found.<sup>35</sup>

In the immediate posttransplant period, certain expected findings should be appreciated; transient anastomotic edema may cause mildly elevated PSV, turbulent flow, and diminished RI.<sup>36</sup> Graft edema may conversely result in increased RI with diminished diastolic flow.<sup>36</sup>

In children, graft thrombosis is the leading cause of transplant loss in the 1st year, accounting for 35% of 1st year losses and 18% of all losses.<sup>37</sup> Arterial thrombosis may be diagnosed by US, noting that hyperacute rejection may be a mimic, and Doppler settings must be optimized for detection of low flow. Venous thrombosis is manifested by the absence of flow in the renal vein as well as high RI or even reversal of flow in the artery; associated graft edema is expected.

Renal artery stenosis is a late vascular complication seen in transplantation. With the exception of two studies that we know of,<sup>38,39</sup>

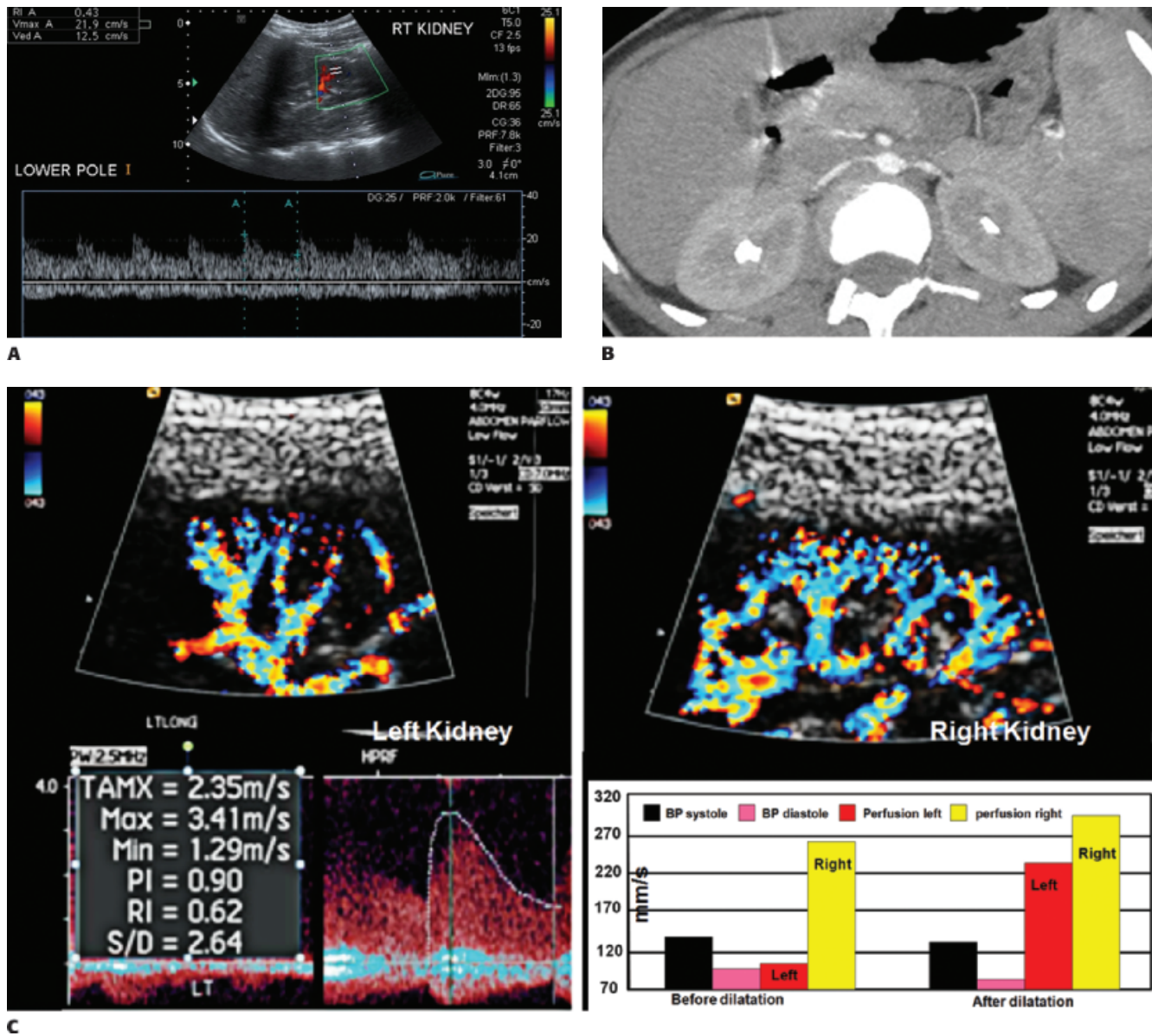


**Figure 35-6.** Renal artery stenosis. Screening US from a 12-year-old female with hypertension (A) shows a RI of 0.43. Oblique axial maximum intensity projection image from CT angiography (B) shows bilateral proximal renal artery stenosis. Findings were confirmed at angiography (not shown); angioplasty was performed with resulting resolution of hypertension. DTPM from a different patient (C) shows the left and right kidneys, respectively. Flow spectrum of the stenotic left renal artery shows a maximum flow velocity of 341 cm/s. DTPM perfusion intensity measurements and diastolic/systolic blood pressure before and after angioplasty are shown on the lower panel.

the work relating to posttransplant arterial stenosis has been performed in adults and extrapolated to children. It is our practice to use the same cutoff values for PSV and renal artery-to-iliac artery ratio as is used in native kidneys: 180 cm/s and 3.5, respectively.

Unfortunately, the common causes of delayed intrinsic graft dysfunction—cyclosporine toxicity, allograft rejection, and acute tubular necrosis—all result in a nonspecific elevation in resistive indices.<sup>36,40</sup>

The role of DTPM in the setting of renal transplant follow-up has been evaluated. A study of 78 adult renal transplant recipients showed a correlation of tissue perfusion measurements with histologic features of peritubular inflammation and interstitial fibrosis.<sup>41</sup> A DTPM study of 38 renal transplants in children and young adults showed a marked decline in cortical perfusion as early as

1 year after transplant.<sup>42</sup> This decline was more marked in the peripheral 50% of the cortex (Fig. 35-7). In parallel, the perfusion pulsatility was rising in these transplants with decreasing cortical perfusion. Moreover, in a recent publication, DTPM was shown to have predictive value in anticipating the survival of transplant function.<sup>43</sup>

### Diabetic Nephropathy

DTPM has been studied in assessing renal microvascular damage in pediatric patients with type 1 diabetes mellitus and apparently normal renal function without microalbuminuria.<sup>44</sup> In a study of 92 pediatric patients as compared to 71 healthy control subjects, it was found that perfusion in the peripheral aspect of the cortex was 31% decreased in the diabetes group relative to controls.

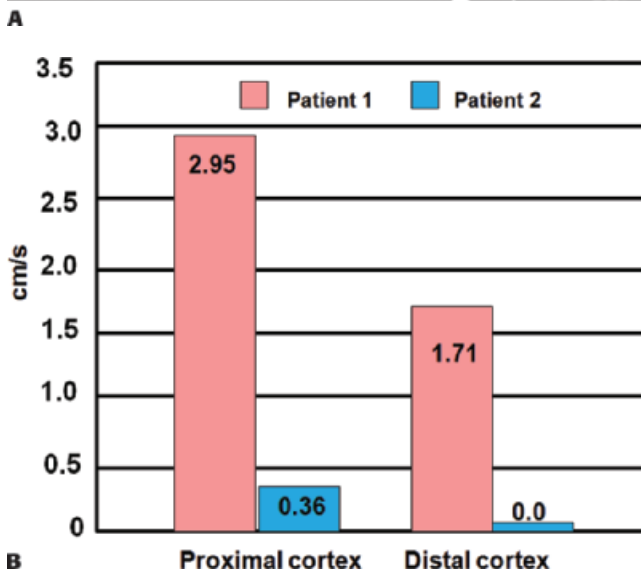
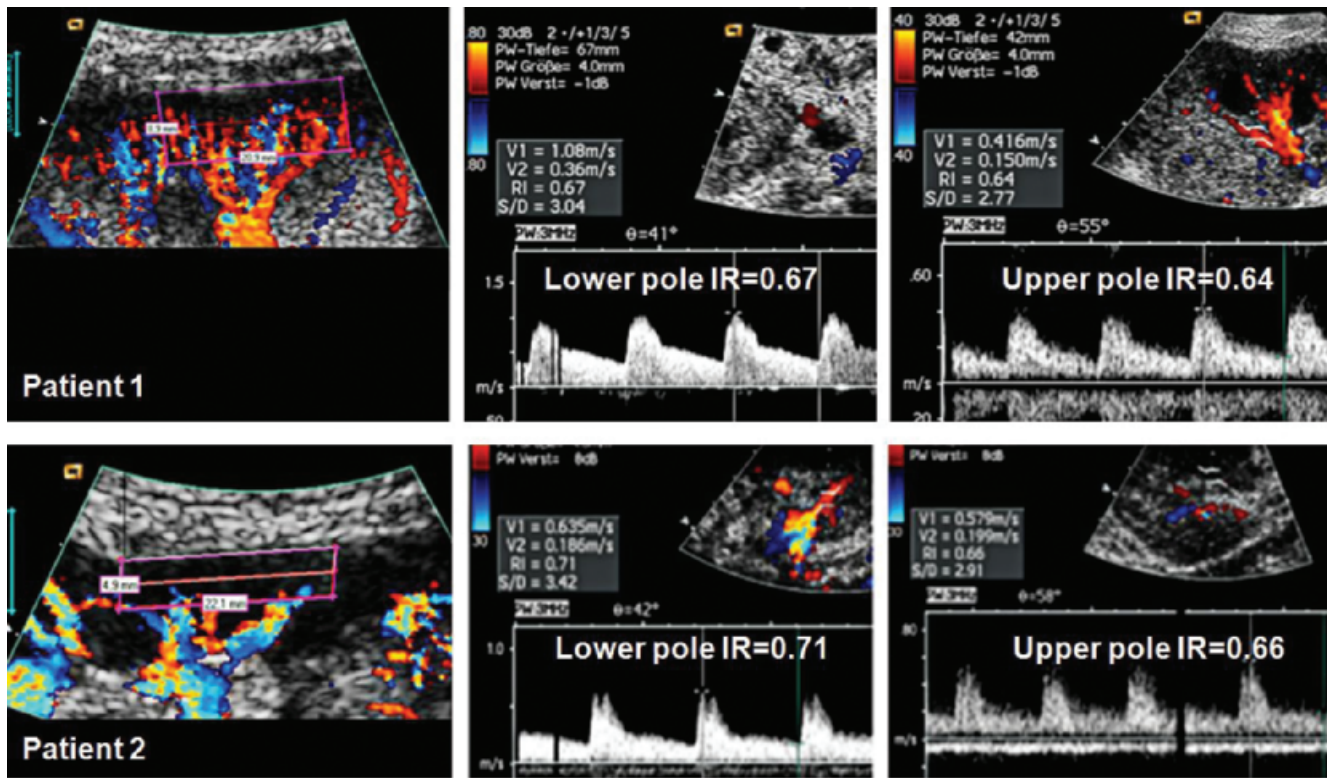


**Figure 35-7.** Comparison of perfusion in two renal transplants with differing function. **A:** Patient 1: Well-functioning transplant with good cortical vascularization and normal serum creatinine. Patient 2: Insufficient transplant with total loss of peripheral cortical microvasculature and elevated creatinine. Resistive indices are similar in both transplants. **B:** Perfusion intensity graph shows the values for the proximal and distal renal cortices of the two patients.

**Bowel**

In clinical practice, evaluation of patients with inflammatory bowel disease relies upon clinical, laboratory, endoscopic, and imaging parameters, as appropriate. Doppler US can play a role in decision making and management. A recent meta-analysis demonstrated no significant difference in the diagnostic accuracy among US, MRI, and CT in the evaluation of patient's with inflammatory bowel disease<sup>45</sup> (Fig. 35-8).

Blood flow in normal pediatric splanchnic arteries has been described. Bowel inflammation results in increased volume of splanchnic blood flow with a concomitant decrease in RI.<sup>46-49</sup> Maconi et al.<sup>49</sup> found no relation between splanchnic

hemodynamics and disease activity, though they do report decreased RI in all patients with Crohn's relative to control subjects. As expected, there is also correlation between the presence of Crohn disease and elevated levels of portal venous blood flow.<sup>49</sup> In their study of 92 pediatric patients, Spalinger et al.<sup>1</sup> found a correlation between vessel density measured in the bowel wall by CDS, bowel wall thickness, and disease activity in Crohn patients.

Contrast-enhanced US in the setting of Crohn's has been well studied, with several potential clinical applications identified. Contrast-enhanced US has proven effective in differentiating hypervascular inflammatory stenoses from hypovascular fibrotic

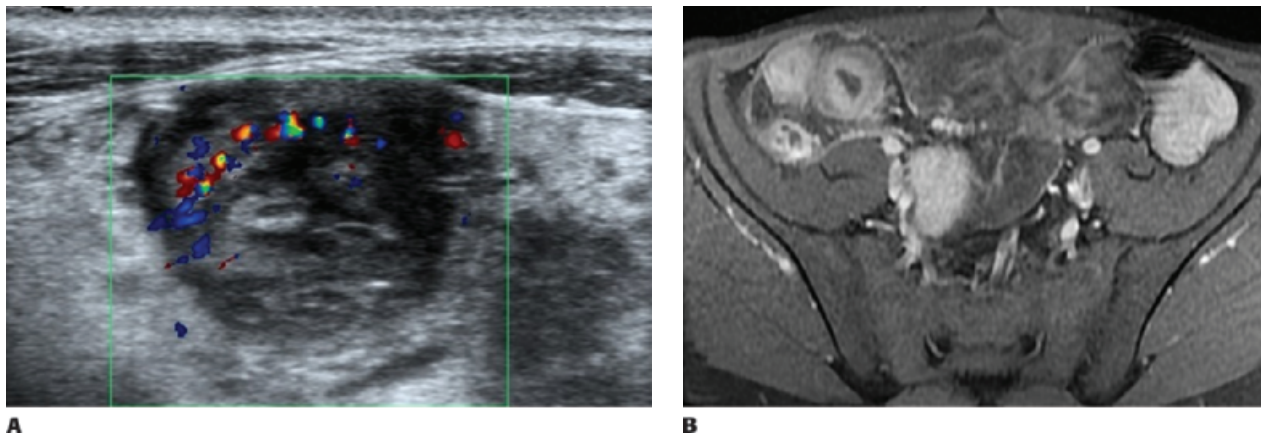


**Figure 35-8.** Crohn disease in a 16-year-old male. **A:** CDS shows hyperemia and mural thickening involving the cecum. **B:** Contrast-enhanced T1 with fat saturation MR sequence shows thickening and hyperenhancement of the terminal ileum, cecum, and appendix.

stenoses.<sup>50</sup> Monitoring treatment effect is also possible by CEUS. Quantitative changes in the pattern of enhancement in successfully treated bowel have been shown after pharmacologic treatment.<sup>51</sup> Further, residual hyperemia of a thickened bowel wall after treatment may portend relapse.<sup>52</sup>

DTPM has been studied in the setting of Crohn disease. In a report of 14 children with Crohn disease as compared to 34 healthy children, it was found that mean flow velocity in regions of diseased small and large bowel were significantly elevated in Crohn patients.<sup>53</sup> Mean small bowel flow velocity in Crohn disease was 0.095 cm/s

versus 0.025 cm/s in control subjects, whereas large bowel mean flow velocity was 0.082 cm/s compared to 0.012 cm/s in healthy controls.

In a study of 12 pediatric patients with ulcerative colitis, colonic wall perfusion as measured by DTPM was significantly correlated with histopathologic changes as diagnosed from biopsy specimens.<sup>54</sup>

Altered mesenteric flow is also present in celiac disease. A study of 23 children found that PSVs in the SMA were higher in untreated celiac patients relative to healthy controls and to treated celiac patients.<sup>55</sup> The PSV in the treated group was found to be similar to that of normal patients.

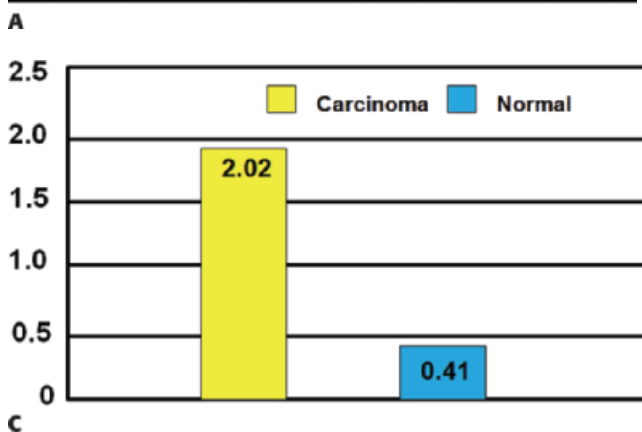
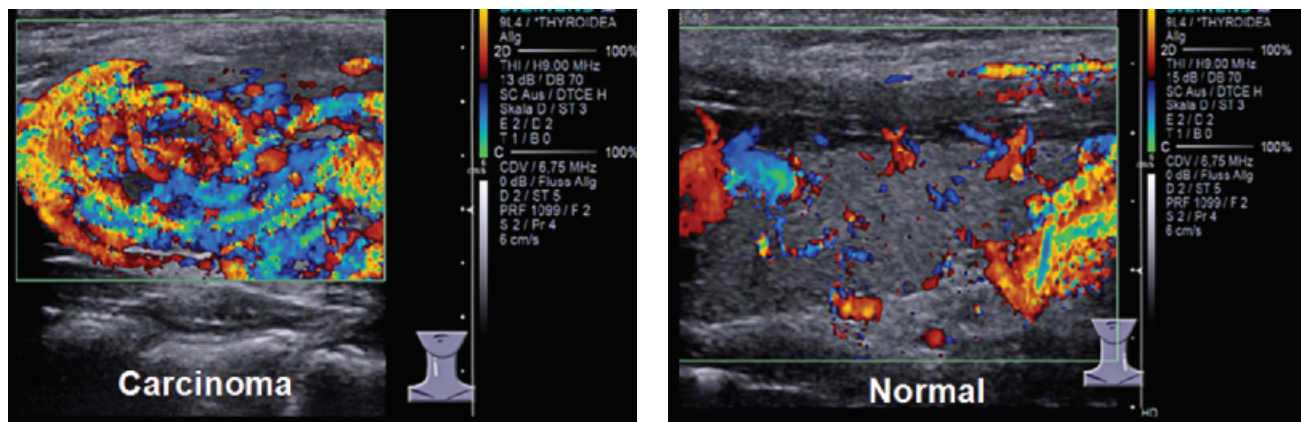


**Figure 35-9.** Perfusion ultrasound in a child with thyroid carcinoma. DTPM demonstrates increased perfusion intensity in thyroid carcinoma (**A**) compared to normal (**B**). **C:** Perfusion intensity in the lesion is measured at 2.02 cm/s, whereas the background thyroid shows a perfusion intensity of 0.41 cm/s.

Please exchange text and insert: Dr. Thomas Scholbach and his son Dr. Jakob Scholbach developed the PixelFlux technique and software and both own the Chameleon Software company.

## 10 Perfusion Imaging in Clinical Practice

### Tumors

Tumor perfusion can be evaluated by DTPM; tumoral ischemia, hypoperfusion, or hyperemia may be revealed (Fig. 35-9). This is potentially important information as tumor hypoxia has been correlated with chemo- and radioresistance of certain tumors.<sup>56-58</sup> In a series of metastatic squamous cell tumors of the head and neck, it was found that tumor perfusion as measured by DTPM was correlated with a direct measure of tumor oxygenation; hypoxic tumors had significantly lower perfusion than normally oxygenated ones.<sup>59</sup>

The clinical application of DTPM in the oncology setting is in the early phases of investigation, with considerable research required before a defined clinical role for DTPM in the routine management of these patients is established.

### Disclosures

Drs. Karl Muchantef and Ricardo Faingold have no disclosures.

~~Dr. Thomas Scholbach helped to develop the concept behind the PixelFlux software and may in the future receive an income. His son, Jakob Scholbach, is owner of PixelFlux Chameleon Software.~~

### REFERENCES

1. Spalinger J, Patriquin H, Miron MC, et al. Doppler US in patients with crohn disease: vessel density in the diseased bowel reflects disease activity. *Radiology* 2000;217(3):787-791.
2. Faingold R, Daneman A, Tomlinson G, et al. Necrotizing enterocolitis: assessment of bowel viability with color doppler US. *Radiology* 2005;235(2):587-594.
3. Schroder RJ, Bostanjoglo M, Hidajat N, et al. Analysis of vascularity in breast tumors—comparison of high frequency ultrasound and contrast-enhanced color harmonic imaging. *Rofa* 2002;174(9):1132-1141.
4. Kawasaki T, Ueo T, Itani T, et al. Vascularity of advanced gastric carcinoma: evaluation by using power doppler imaging. *J Gastroenterol Hepatol* 2001;16(2):149-153.
5. Kuwa T, Cancio LC, Sondeen JL, et al. Evaluation of renal cortical perfusion by noninvasive power doppler ultrasound during vascular occlusion and reperfusion. *J Trauma* 2004;56(3):618-624.
6. Lassau N, Koscielny S, Opolon P, et al. Evaluation of contrast-enhanced color doppler ultrasound for the quantification of angiogenesis in vivo. *Invest Radiol* 2001;36(1):50-55.
7. Ogura O, Takebayashi Y, Sameshima T, et al. Preoperative assessment of vascularity by color Doppler ultrasonography in human rectal carcinoma. *Dis Colon Rectum* 2001;44(4):538-546; discussion 546-538.
8. Stoeckelhuber BM, Wiesmann M, Kreft B, et al. Perfusion imaging of the kidney using contrast-enhanced phase-inversion ultrasound. *Rontgenpraxis* 2004;55(5):167-174.
9. Krix M, Weber MA, Krakowski-Roosen H, et al. Assessment of skeletal muscle perfusion using contrast-enhanced ultrasonography. *J Ultrasound Med* 2005;24(4):431-441.
10. Siegel MJ. *Pediatric sonography*. 4th ed. Lippincott Williams & Wilkins; 2011.
11. Boote EJ. AAPM/RSNA physics tutorial for residents: topics in US: doppler US techniques: concepts of blood flow detection and flow dynamics. *Radiographics* 2003;23(5):1315-1327.
12. Perrella RR, Duerinckx AJ, Tessler FN, et al. Evaluation of renal transplant dysfunction by duplex doppler sonography: a prospective study and review of the literature. *Am J Kidney Dis* 1990;15(6):544-550.
13. Taylor GA. Potential pediatric applications for US contrast agents: lessons from the laboratory. *Pediatr Radiol* 2000;30(2):101-109.
14. Fleischer AC, Niermann KJ, Donnelly EF, et al. Sonographic depiction of microvessel perfusion: principles and potential. *J Ultrasound Med* 2004;23(11):1499-1506.
15. Darge K. Contrast-enhanced US (CEUS) in children: ready for prime time in the United States. *Pediatr Radiol* 2011;41(11):1486-1488.
16. Chameleon-Software. PixelFlux. <http://www.chameleon-software.de>
17. Chavhan GB, Parra DA, Mann A, et al. Normal Doppler spectral waveforms of major pediatric vessels: specific patterns. *Radiographics* 2008;28(3):691-706.
18. Ilves P, Lintrop M, Talvik I, et al. Changes in cerebral and visceral blood flow velocities in asphyxiated term neonates with hypoxic-ischemic encephalopathy. *J Ultrasound Med* 2009;28:1471-1480.
19. Faingold R, Cassia GS, Saint-Martin C. Cerebral perfusion measurements using dynamic color doppler sonography in neonates with Hypoxic Ischemic Encephalopathy (HIE) treated with therapeutic hypothermia. *Pediatric Radiol* 2011;(1):S250-S310. NE252-NE253.
20. Cassia GS, Faingold R, Bernard C, et al. Neonatal hypoxic-ischemic injury: sonography and dynamic color Doppler sonography perfusion of the brain and abdomen with pathologic correlation. *AJR Am J Roentgenol* 2012;199(6):W743-W752.
21. Cassia GS, Faingold R. Hypoxic ischemic injury: intestinal appearances and perfusion measurements using ultrasound and dynamic color doppler sonography in neonates submitted to therapeutic hypothermia. *Pediatric Radiol* 2011;41(1):S250-S310. FN259.
22. Allison JW, Faddis LA, Kinder DL, et al. Intracranial resistive index (RI) values in normal term infants during the first day of life. *Pediatr Radiol* 2000;30(9):618-620.
23. Liu J, Cao HY, Huang XH, et al. The pattern and early diagnostic value of Doppler ultrasound for neonatal hypoxic-ischemic encephalopathy. *J Trop Pediatr* 2007;53(5):351-354.
24. Kuzmic AC, Brkljacic B, Ivankovic D, et al. Doppler sonographic renal resistance index in healthy children. *Eur Radiol* 2000;10(10):1644-1648.
25. Vade A, Subbaiah P, Kalbhen CL, et al. Renal resistive indices in children. *J Ultrasound Med* 1993;12(11):655-658.
26. Robitaille P, Lord H, Dubois J, et al. A large unilateral renal artery aneurysm in a young child. *Pediatr Radiol* 2004;34(3):253-255.
27. Park SH, Chi JG, Choi Y. Primary intimal fibroplasia with multiple aneurysms of renal artery in childhood. *Child Nephrol Urol* 1990;10(1):51-55.
28. Bartosh SM, Aronson AJ. Childhood hypertension. An update on etiology, diagnosis and treatment. *Pediatr Clin North Am* 1999;46(2):235-252.
29. Kliever MA, Hertzberg BS, Keogan MT, et al. Early systole in the healthy kidney: variability of Doppler US waveform parameters. *Radiology* 1997;205(1):109-113.
30. Kliever MA, Tupler RH, Carroll BA, et al. Renal artery stenosis: analysis of Doppler waveform parameters and tardus-parvus pattern. *Radiology* 1993;189(3):779-787.
31. Kurian J, Epelman M, Darge K, et al. The role of CT angiography in the evaluation of pediatric renovascular hypertension. *Pediatr Radiol* 2013;43(4):490-501; quiz 487-499.
32. Castelli PK, Dillman JR, Kershaw DB, et al. Renal sonography with Doppler for detecting suspected pediatric renin-mediated hypertension—is it adequate? *Pediatr Radiol* 2014;44(1):42-49.
33. Ciccone MM, Cortese F, Fiorella A, et al. The clinical role of contrast-enhanced ultrasound in the evaluation of renal artery stenosis and diagnostic superiority as compared to traditional echo-color-Doppler flow imaging. *Int Angiol* 2011;30(2):135-139.
34. Melany ML, Grant EG, Duerinckx AJ, et al. Ability of a phase shift US contrast agent to improve imaging of the main renal arteries. *Radiology* 1997;205(1):147-152.
35. Gholami S, Sarwal MM, Naesens M, et al. Standardizing resistive indices in healthy pediatric transplant recipients of adult-sized kidneys. *Pediatr Transplant* 2010;14(1):126-131.
36. Nixon JN, Biyyam DR, Stanescu L, et al. Imaging of pediatric renal transplants and their complications: a pictorial review. *Radiographics* 2013;33(5):1227-1251.
37. Smith JM, Stablein D, Singh A, et al. Decreased risk of renal allograft thrombosis associated with interleukin-2 receptor antagonists: a report of the NAPRTCS. *Am J Transplant* 2006;6(3):585-588.
38. del Valle SY, Lorente Ramos RM, Berrocal Frutos T, et al. Vascular complications in pediatric renal transplant: echographic diagnosis. *An Esp Pediatr* 1999;50(3):263-268.
39. Toma P, Lucigrai G, Magnano G, et al. Intraparenchymal renal Doppler: the indirect signs of renal artery stenosis in native and transplanted kidneys in childhood. *Radiol Med* 1994;88(3):244-248.
40. Coley BD. Pediatric applications of abdominal vascular Doppler: Part II. *Pediatr Radiol* 2004;34(10):772-786.
41. Scholbach T, Wang HK, Yang AH, et al. Correlation of histopathology and dynamic tissue perfusion measurement (DTPM) in renal transplants. Paper presented at ERA-EDTA Congress 2011.

Q5

Q6

meanwhile the paper was published in an open access journal: BMC Nephrology 2013, 14:143 - <http://www.biomedcentral.com/1471-2369/14/143>

42. **Scholbach T, Girelli E, Scholbach J.** Tissue pulsatility index: a new parameter to evaluate renal transplant perfusion. *Transplantation* 2006;81(5):751–755.
43. **Scholbach T, Wang HK, Yang AH, et al.** Prognostic value of dynamic tissue perfusion measurements in transplanted kidneys. *Open J Organ Transplant Surg* 2014;4:1–5.
44. **Scholbach T, Vogel C, Bergner N.** Color doppler sonographic dynamic tissue perfusion measurement demonstrates significantly reduced cortical perfusion in children with diabetes mellitus type 1 without microalbuminuria and apparently healthy kidneys. *Ultraschall Med* 2014;35(5):445–450.
45. **Horsthuis K, Bipat S, Bennink RJ, et al.** Inflammatory bowel disease diagnosed with US, MR, scintigraphy, and CT: meta-analysis of prospective studies. *Radiology* 2008;247(1):64–79.
46. **Sjekavica I, Barbaric-Babic V, Krznaric Z, et al.** Assessment of Crohn's disease activity by doppler ultrasound of superior mesenteric artery and mural arteries in thickened bowel wall: cross-sectional study. *Croat Med J* 2007;48(6):822–830.
47. **Di Sabatino A, Armellini E, Corazza GR.** Doppler sonography in the diagnosis of inflammatory bowel disease. *Dig Dis* 2004;22(1):63–66.
48. **Sigirci A, Baysal T, Kutlu R, et al.** Doppler sonography of the inferior and superior mesenteric arteries in ulcerative colitis. *J Clin Ultrasound* 2001;29(3):130–139.
49. **Maconi G, Parente F, Bollani S, et al.** Factors affecting splanchnic haemodynamics in Crohn's disease: a prospective controlled study using Doppler ultrasound. *Gut* 1998;43(5):645–650.
50. **Kratzer W, von Tirpitz C, Mason R, et al.** Contrast-enhanced power Doppler sonography of the intestinal wall in the differentiation of hypervascularized and hypovascularized intestinal obstructions in patients with Crohn's disease. *J Ultrasound Med* 2002;21(2):149–157; quiz 158–149.
51. **Quaia E, Migaleddu V, Baratella E, et al.** The diagnostic value of small bowel wall vascularity after sulfur hexafluoride-filled microbubble injection in patients with Crohn's disease. Correlation with the therapeutic effectiveness of specific anti-inflammatory treatment. *Eur J Radiol* 2009;69(3):438–444.
52. **Ripolles T, Martinez MJ, Barrachina MM.** Crohn's disease and color Doppler sonography: response to treatment and its relationship with long-term prognosis. *J Clin Ultrasound* 2008;36(5):267–272.
53. **Scholbach T, Herrero I, Scholbach J.** Dynamic color Doppler sonography of intestinal wall in patients with Crohn disease compared with healthy subjects. *J Pediatr Gastroenterol Nutr* 2004;39(5):524–528.
54. **Scholbach T, Hormann J, Scholbach J.** Dynamic tissue perfusion measurement in the intestinal wall—correlation with ulcerative colitis. *J Med Ultrasound* 2010;18(2):62–70.
55. **Ertem D, Tuney D, Baloglu H, et al.** Superior mesenteric artery blood flow in children with celiac disease. *J Pediatr Gastroenterol Nutr* 1998;26(2):140–145.
56. **Lin SC, Chien CW, Lee JC, et al.** Suppression of dual-specificity phosphatase-2 by hypoxia increases chemoresistance and malignancy in human cancer cells. *J Clin Invest* 2011;121(5):1905–1916.
57. **Wen YA, Stevens PD, Gasser ML, et al.** Downregulation of PHLPP expression contributes to hypoxia-induced resistance to chemotherapy in colon cancer cells. *Mol Cell Biol* 2013;33(22):4594–4605.
58. **Wu YC, Ling TY, Lu SH, et al.** Chemotherapeutic sensitivity of testicular germ cell tumors under hypoxic conditions is negatively regulated by SENP1-controlled sumoylation of OCT4. *Cancer Res* 2012;72(19):4963–4973.
59. **Scholbach T, Scholbach J, Krombach GA, et al.** New method of dynamic color doppler signal quantification in metastatic lymph nodes compared to direct polarographic measurements of tissue oxygenation. *Int J Cancer* 2005;114(6):957–962.

Scientific title and academic degrees of Thomas Scholbach are:  
Prof. Dr. med. habil. Thomas Scholbach; I'm a professor of pediatrics at  
the Dresden University, Dresden Germany

#### Queries

- [Q1] Please provide details of degrees for all the three contributing authors.
- [Q2] Please check whether the section level headings identified are correct.
- [Q3] Please check whether the deletion of “and” in the sentence beginning “Spectral Doppler velocity measurements ...” is okay.
- [Q4] Please check whether the edits made to the sentence beginning “Mean perfusion intensity thus als...” are okay.
- [Q5] Please provide publisher location for the reference no. 10.
- [Q6] Please provide conference location and conference date for the reference no. 41.

"yes, it's o.k."  
(T.S.)

"yes, it's o.k."  
(T.S.)